

Missense mutation in immunodeficient patients shows the multifunctional roles of coiled-coil domain 3 (CC3) in STIM1 activation

Mate Maus^{a,1}, Amit Jairaman^{b,1}, Peter B. Stathopoulos^{c,d}, Martin Muik^e, Marc Fahrner^e, Carl Weidinger^a, Melina Benson^a, Sebastian Fuchs^{f,g}, Stephan Ehlf^{f,h}, Christoph Romanin^e, Mitsuhiro Ikura^c, Murali Prakriya^b, and Stefan Feske^{a,2}

^aDepartment of Pathology, New York University School of Medicine, New York, NY 10016; ^bDepartment of Pharmacology, Northwestern University Feinberg School of Medicine, Chicago, IL 60611; ^cPrincess Margaret Cancer Centre and Department of Medical Biophysics, University of Toronto, Toronto, ON, Canada, M5G 1L7; ^dDepartment of Physiology and Pharmacology, Schulich School of Medicine and Dentistry, Western University, London, ON, Canada, N6A 5C1; ^eInstitute of Biophysics, Johannes Kepler University Linz, A-4020 Linz, Austria; ^fCenter for Chronic Immunodeficiency, University Medical Center, University of Freiburg, D-79106 Freiburg, Germany; ^gFaculty of Biology, University of Freiburg, D-79104 Freiburg, Germany; and ^hCenter for Pediatrics and Adolescent Medicine, University Medical Center, University of Freiburg, D-79106 Freiburg, Germany

Edited by Richard S. Lewis, Stanford University School of Medicine, Stanford, CA, and accepted by the Editorial Board March 27, 2015 (received for review October 1, 2014)

Store-operated Ca^{2+} entry (SOCE) is a universal Ca^{2+} influx pathway that is important for the function of many cell types. SOCE occurs upon depletion of endoplasmic reticulum (ER) Ca^{2+} stores and relies on a complex molecular interplay between the plasma membrane (PM) Ca^{2+} channel ORAI1 and the ER Ca^{2+} sensor stromal interaction molecule (STIM) 1. Patients with null mutations in *ORAI1* or *STIM1* genes present with severe combined immunodeficiency (SCID)-like disease. Here, we describe the molecular mechanisms by which a loss-of-function *STIM1* mutation (R429C) in human patients abolishes SOCE. R429 is located in the third coiled-coil (CC3) domain of the cytoplasmic C terminus of STIM1. Mutation of R429 destabilizes the CC3 structure and alters the conformation of the STIM1 C terminus, thereby releasing a polybasic domain that promotes STIM1 recruitment to ER-PM junctions. However, the mutation also impairs cytoplasmic STIM1 oligomerization and abolishes STIM1-ORAI1 interactions. Thus, despite its constitutive localization at ER-PM junctions, mutant STIM1 fails to activate SOCE. Our results demonstrate multifunctional roles of the CC3 domain in regulating intra- and intermolecular STIM1 interactions that control (i) transition of STIM1 from a quiescent to an active conformational state, (ii) cytoplasmic STIM1 oligomerization, and (iii) STIM1-ORAI1 binding required for ORAI1 activation.

STIM1 | calcium | ORAI1 | immunodeficiency | mutation

Store-operated Ca^{2+} entry (SOCE) is mediated by Ca^{2+} release-activated Ca^{2+} (CRAC) channels in the plasma membrane (PM) that are formed by multimers of ORAI proteins, which constitute the permeation pore of the channel (1–4). The opening of ORAI channels is mediated by stromal interaction molecule (STIM) 1 and STIM2, single pass transmembrane proteins whose N and C termini are located in the endoplasmic reticulum (ER) lumen and cytoplasm, respectively (5, 6). STIM1 and STIM2 are activated after depletion of ER Ca^{2+} stores in response to ligation of cell surface receptors that mediate phospholipase C (PLC) activation. The importance of SOCE is emphasized by null and loss-of-function mutations in *ORAI1* and *STIM1* genes, which cause a disease syndrome called CRAC channelopathy that is characterized by immunodeficiency, autoimmunity, ectodermal dysplasia, and skeletal myopathy (7).

SOCE is a highly choreographed process that involves a complex conformational rearrangement of STIM1 proteins, their oligomerization in the ER lumen and in the cytoplasm, and subsequent translocation from the bulk ER to ER-PM junctions (4, 8). There, STIM1 oligomers form puncta and bind ORAI1. SOCE is initiated by dissociation of Ca^{2+} from a paired EF-hand (EFh) domain in the ER luminal N terminus of STIM1 after store depletion (Fig. 1A) and association of STIM1 N termini. These events result in a conformational extension of the cytoplasmic

C terminus of STIM1 (STIM-CT) (9–12) and exposure of a polybasic domain at the distal end of STIM1-CT. The polybasic domain interacts with acidic phospholipids in the PM, thereby facilitating recruitment of STIM1 oligomers to ER-PM junctions (9–11, 13) and subsequent binding of ORAI1. The STIM1-CT contains three coiled-coil (CC) domains: CC1 (amino acids 247–336), CC2 (amino acids 345–391), and CC3 (amino acids 408–437) (Fig. 1A). CC2 and CC3 are part of an ~100-aa region in STIM1-CT that is variously termed CRAC activation domain (CAD, amino acids 342–448) (14), STIM1-ORAI1 activating region (SOAR, amino acids 344–442) (15), or coiled-coil domain b9 (CCb9, amino acids 339–446) (16). CAD mediates the dimerization of STIM1 C termini (17) and the higher order oligomerization of STIM1 dimer units (18). CAD is sufficient to activate CRAC channels and to induce constitutive Ca^{2+} influx by binding to ORAI1 (14–16). The structurally best defined region in CAD is CC2 that establishes the binding interactions with ORAI1 (19). By contrast, the role of CC3 remains to be elucidated.

Significance

Stromal interaction molecule (STIM) 1 is an essential activator of the ORAI1 calcium (Ca^{2+}) channel that mediates Ca^{2+} entry into many cell types. Patients with mutations in *STIM1* or *ORAI1* genes suffer from a severe immunodeficiency syndrome. Here, we studied a disease-causing mutant of STIM1 that is incapable of activating ORAI1 channels, thereby uncovering key molecular mechanisms of STIM1 function. The autosomal recessive R429C mutation interferes with the structural integrity of a protein-protein interaction domain in STIM1 and impairs the ability of STIM1 to multimerize and bind to ORAI1. Drugs targeting this domain may provide a means to selectively modulate STIM1-ORAI1 interaction and Ca^{2+} entry as a novel approach to treat autoimmune diseases and other disorders associated with abnormal ORAI1-mediated Ca^{2+} entry.

Author contributions: M. Maus, A.J., P.B.S., M. Muik, M.F., C.W., S. Fuchs, S.E., C.R., M.I., M.P., and S. Feske designed research; M. Maus, A.J., P.B.S., M. Muik, M.F., C.W., M.B., and S. Fuchs performed research; M. Maus, A.J., P.B.S., C.R., M.I., and S. Feske contributed new reagents/analytic tools; M. Maus, A.J., P.B.S., M. Muik, M.F., C.W., S. Fuchs, S.E., C.R., M.I., M.P., and S. Feske analyzed data; and M. Maus, A.J., P.B.S., C.R., M.I., M.P., and S. Feske wrote the paper.

Conflict of interest statement: S. Feske is a cofounder of Calcimedica.

This article is a PNAS Direct Submission. R.S.L. is a guest editor invited by the Editorial Board.

¹M. Maus and A.J. contributed equally to this work.

²To whom correspondence should be addressed. Email: feskes01@nyumc.org.

This article contains supporting information online at www.pnas.org/lookup/suppl/doi:10.1073/pnas.1418852112/-DCSupplemental.

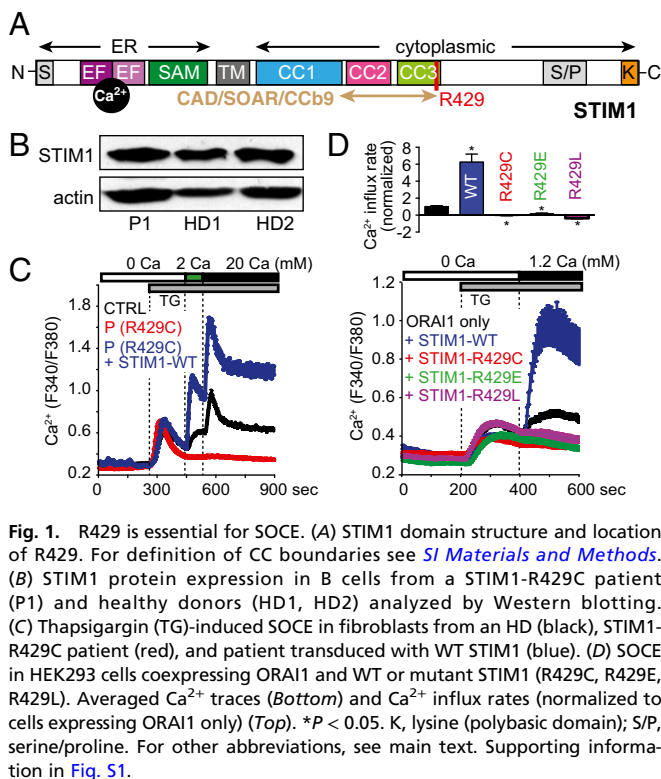


Fig. 1. R429 is essential for SOCE. (A) STIM1 domain structure and location of R429. For definition of CC boundaries see *SI Materials and Methods*. (B) STIM1 protein expression in B cells from a STIM1-R429C patient (P1) and healthy donors (HD1, HD2) analyzed by Western blotting. (C) Thapsigargin (TG)-induced SOCE in fibroblasts from an HD (black), STIM1-R429C patient (red), and patient transduced with WT STIM1 (blue). (D) SOCE in HEK293 cells coexpressing ORAI1 and WT or mutant STIM1 (R429C, R429E, R429L). Averaged Ca^{2+} traces (Bottom) and Ca^{2+} influx rates (normalized to cells expressing ORAI1 only) (Top). * $P < 0.05$. K, lysine (polybasic domain); S/P, serine/proline. For other abbreviations, see main text. Supporting information in Fig. S1.

We recently described the first patients with CRAC channelopathy due to a loss-of-function mutation in *STIM1* (20). In these patients, a missense mutation (R429C) is located at the distal end of CC3 within CAD (Fig. 1A). We here show that mutation of R429 interferes with multiple distinct functions of STIM1 by destabilizing the structure of CC3 and impairing intra- and intermolecular STIM1 protein interactions. Mutation of R429 results in conformational extension of STIM1-CT and release of the STIM1 polybasic domain that promotes constitutive STIM1 translocation to ER-PM junctions. In addition, mutation of R429 impairs oligomerization of STIM1-CT and STIM1 binding to ORAI1, thereby abolishing CRAC channel activation. We conclude that R429 and CC3 play multiple important roles in STIM1 function and activation of SOCE.

Results

R429 Is Essential for SOCE. Patients homozygous for the R429C missense mutation in the CC3 domain of *STIM1* (Fig. 1A) suffer from typical CRAC channelopathy (20). STIM1 expression in patient B cells and fibroblasts was modestly reduced compared with healthy donors (Fig. 1B and Fig. S1A–D). Despite significant STIM1 expression, however, SOCE in patient fibroblasts was abolished (Fig. 1C) similar to loss of SOCE in their T cells (20). T cells from the patient’s parents, who are heterozygous for the R429C mutation (20), showed partially reduced SOCE although parents were clinically asymptomatic and had a normal immune phenotype in vitro (Table S1). SOCE in the patient fibroblasts could be fully restored by overexpression of WT STIM1 (STIM1-WT) (Fig. 1C). Defective SOCE in the patient’s cells was not specific to the cysteine substitution in STIM1-R429C and putative formation of disulfide bonds because coexpression of either STIM1-R429C, -R429E, or -R429L together with ORAI1 failed to enhance SOCE in HEK293 cells in contrast to STIM1-WT (Fig. 1D). In fact, expression of all STIM1 mutants suppressed SOCE below endogenous levels (Fig. 1D). This suppression is due to a dominant negative effect of STIM1 mutants on SOCE, which we confirmed by co-overexpression of

WT and mutant STIM1 (Fig. S1E and F). These results show that mutation of R429 abolishes STIM1 function.

Mutation of R429 Abolishes STIM1 Interactions with ORAI1. R429 is located in the CC3 domain of CAD, the minimal activating domain of STIM1 (Fig. 1A). Although CAD is essential for STIM1 binding to ORAI1, the role of CC3 in CAD-ORAI1 interaction is not well defined. To investigate whether mutation of R429 interferes with STIM1-ORAI1 binding, we measured fluorescence resonance energy transfer (FRET) between ORAI1-YFP and either WT or mutant (R429C) STIM1-CFP in HEK293 cells. Depletion of ER Ca^{2+} stores induced an approximately twofold increase in E-FRET between STIM1-WT and ORAI1 (Fig. 2A and B), consistent with STIM1-ORAI1 coupling described previously (18, 21, 22). By contrast, no increase in E-FRET was observed in cells coexpressing ORAI1 and STIM1-R429C, suggesting that mutation of R429 interferes with STIM1-ORAI1 binding after store depletion (Fig. 2A and B). Exogenous expression of the CAD/CCb9 domain along with ORAI1 has been shown to result in constitutive colocalization and binding of CAD/CCb9 to ORAI1 (14, 16). Accordingly, we observed robust resting E-FRET between ORAI1-CFP and WT YFP-CAD (Fig. 2C). By contrast, E-FRET between ORAI1-CFP and mutant YFP-CAD-R429C was strongly reduced. Likewise, confocal microscopy showed that YFP-CAD-WT was predominantly found at the PM as expected whereas YFP-CAD-R429C was localized in the cytoplasm, indicating reduced binding of CAD-R429C to ORAI1 (Fig. 2D). To investigate whether the R429C mutation abolishes CRAC channel activation by CAD, we coexpressed ORAI1 and WT or mutant mCherry-tagged Ccb9 (which behaves like CAD) (16) in HEK293 cells. Whereas mCherry-CCb9-WT resulted in strong constitutive Ca^{2+} influx, mutant mCherry-CCb9-R429C failed to induce Ca^{2+} influx (Fig. 2E). Taken together, these data show that R429 in CC3 is required for STIM1-ORAI1 binding and CRAC channel activation.

Mutation of R429 Does Not Impair Dimerization of CAD. Previous studies have shown that STIM1 fragments containing the CAD/SOAR are detected in vitro as dimers (10, 17, 19). The crystal

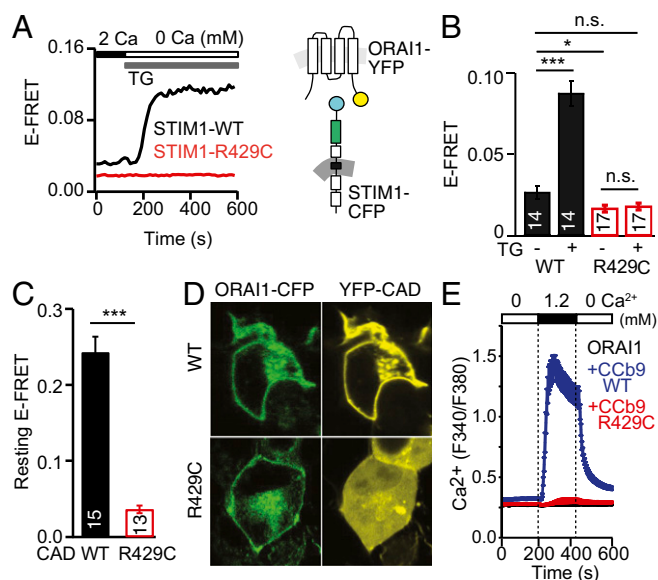


Fig. 2. R429 mutation abolishes STIM1-ORAI1 interaction. (A) Representative E-FRET traces between WT or mutant STIM1-CFP and ORAI1-YFP in HEK293 cells. (B) Averaged E-FRET before and after stimulation with 1 μ M TG. (C and D) E-FRET (C) and representative confocal images (D) of ORAI1-CFP and WT or mutant (R429C) YFP-CAD expressed in HEK293 cells without TG stimulation in 0 mM Ca^{2+} . (E) Ca^{2+} influx in HEK293 cells coexpressing ORAI1 and WT or mutant (R429C) Ccb9. Numbers of cells analyzed are indicated. * $P < 0.05$; *** $P < 0.001$.

structure of SOAR suggests that R429 is part of the dimerization interface and forms hydrogen bonds with T354 on the second dimer subunit (17). To investigate whether mutation of R429 impairs STIM1 dimerization, we first tested whether expression of STIM1 double mutants, with complementary amino acids at positions 429 and 354 that are capable of forming covalent (C/C), charged (E/R), or hydrophobic (L/L) interactions, restores SOCE. Ectopic expression of STIM1-R429C/T354C, STIM1-R429L/T354L, or STIM1-R429E/T354R in STIM1-deficient fibroblasts (Fig. S24) or coexpression of double mutants with ORAI1 in HEK293 cells (Fig. S2B) failed to rescue and enhance SOCE, respectively. Likewise, double mutant CCb9 constructs, unlike CCb9-WT, were unable to mediate constitutive Ca^{2+} influx in HEK293 cells (Fig. S2C). To further test whether R429 is required for homotypic interactions of CAD, we transfected cells with CFP- and YFP-tagged WT or mutant CAD domains. Levels of resting E-FRET were comparable between WT-WT, WT-R429C, and R429C-R429C CAD domains, indicating that the mutation does not affect CAD dimerization (Fig. 3A). Similarly, when we investigated recombinant STIM1 fragments (amino acids 312–491 and amino acids 234–491) that contain CAD by size exclusion chromatography-multiangle laser light scattering (SEC-MALS), the observed MALS molecular weights for WT and mutant (R429C, R429A, and R429L) proteins corresponded to twice the theoretical molecular weights of the monomeric proteins (Fig. 3B and Fig. S3). Together, these results indicate that R429 is dispensable for the dimerization of STIM1-CT.

R429 Regulates the C-Terminal Oligomerization of STIM1 Dimers. STIM1 has been suggested to form dimers in cells with filled ER Ca^{2+} stores that further oligomerize after ER store depletion (8). We investigated whether R429 regulates this oligomerization of STIM1 dimers by performing coimmunoprecipitation (co-IP) experiments between mutant and WT STIM1. Coexpression of mCherry-STIM1-WT and YFP-STIM1-WT proteins resulted in robust co-IP whereas strongly reduced or no binding was detected between mutant STIM1-R429C proteins or WT and mutant proteins (Fig. 4A). Impaired co-IP was not specific to the R429C mutation because STIM1-R429E and STIM1-R429L proteins, which display defective STIM1 function, also showed reduced binding to WT STIM1 (Fig. S4A). To test whether R429 mediates interaction between STIM1 C termini, we coimmunoprecipitated full-length STIM1 with the soluble STIM1-CT. Whereas WT STIM1-CT was able to bind full-length STIM1-WT, it failed to bind full-length STIM1-R429C, and, conversely, the mutant (R429C) STIM1-CT was unable to co-IP either full-length STIM1-WT or STIM1-R429C (Fig. S4B). A similar defect was observed when we used a recombinant C-terminal STIM1 fragment (amino acids 251–535) containing the R429C mutation to pull down full-length STIM1 (Fig. S4C). Considering that dimerization of mutant STIM1

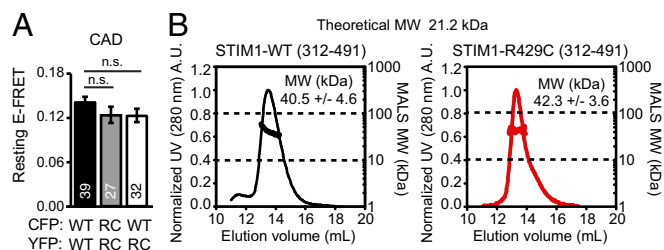


Fig. 3. R429 is not required for CAD and STIM1-CT dimerization. (A) Resting E-FRET between WT and mutant (R429C) CFP- and YFP-tagged STIM1 CAD domains (amino acids 342–448) in nonstimulated HEK293 cells. Numbers of cells analyzed are indicated. (B) WT or mutant (R429C) STIM1 protein fragments (amino acids 312–491) were analyzed by size exclusion chromatography with multiangle laser light scattering (SEC-MALS). The averaged MALS molecular masses (MW) through the major elution peak for WT and R429C proteins are ~ 40 – 42 ± 3.6 – 4.6 kDa. Supporting information in Fig. S3.

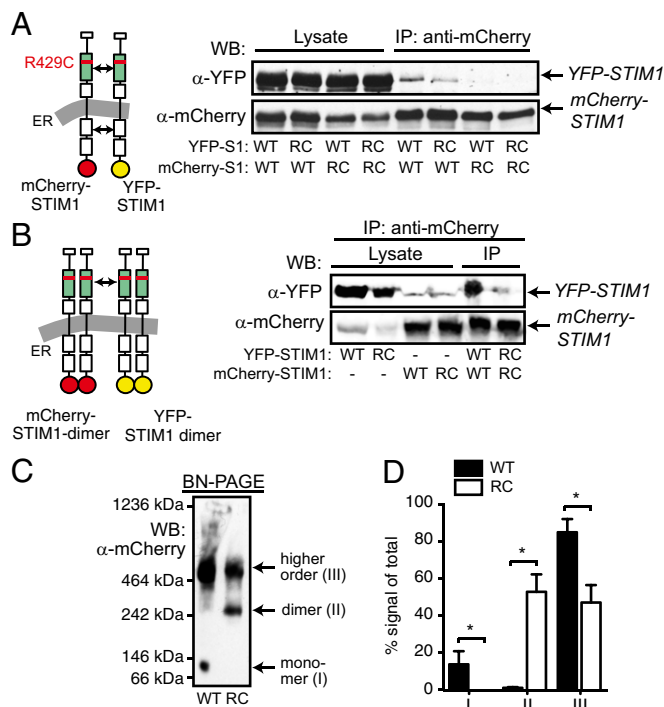


Fig. 4. Mutation of R429 impairs homotypic C-terminal STIM1 interactions. (A) Co-IP of WT and mutant (RC for R429C) full-length YFP-STIM1 and mCherry-STIM1 proteins that were coexpressed in HEK293 cells. (B) Co-IP of WT and mutant full-length mCherry-STIM1 and YFP-STIM1 dimers expressed separately in HEK293 cells. (C) BN-PAGE and Western blot of mCherry-STIM1-WT and mCherry-STIM1-R429C harvested from thapsigargin-stimulated HEK293 cells. (D) Percent densitometric signal intensity per complex averaged from four experiments similar to that shown in C. * $P < 0.05$. Supporting information in Figs. S4 and S5.

C-terminal domains is not impaired (Fig. 3), these data suggest that R429 controls the oligomerization of STIM1 dimers. To test this conclusion further, we used a modified co-IP protocol in which mCherry-tagged STIM1 (WT or R429C) and YFP-tagged STIM1 (WT or R429C) were expressed separately in HEK293 cells, thereby allowing the formation of WT or mutant dimers of only one kind in the same cell. Cell lysates were then mixed to allow oligomerization of dimers and were used for co-IP. Whereas mCherry-STIM1-WT dimers robustly bound YFP-STIM1-WT dimers, interaction between mutant dimers was strongly diminished (Fig. 4B).

To directly test the role of R429 in the formation of STIM1 oligomers, we performed blue-native (BN) PAGE using lysates of HEK293 cells expressing WT or mutant STIM1. The majority of mCherry-STIM1-WT ran at a molecular mass of ≥ 500 kDa, corresponding to at least four times the expected size of an mCherry-STIM1-WT monomer (Fig. 4C and D). By contrast, mCherry-STIM1-R429C complexes ran at two distinct molecular masses. The larger complex was ≥ 500 kDa in size, similar to the mCherry-STIM1-WT complex, whereas the smaller complex was ~ 250 kDa in size (Fig. 4C and D). These results suggest that, whereas the large majority of WT STIM1 readily oligomerizes, mutant STIM1 is impaired in the formation of higher order oligomers, with at least 50% of mutant STIM1 restricted to a dimeric state (Fig. 4C and D). It is noteworthy that STIM1 detected in BN-PAGE and co-IP experiments represents the oligomerized form of STIM1 because thapsigargin (TG) stimulation had no further effect on STIM1 oligomerization (Fig. S4D and E), which is most likely due to the disruption of the ER during cell lysis that is expected to release Ca^{2+} and activate STIM1. We found a similar effect of R429 on STIM1 oligomerization when we used an ER membrane-tethered form of

CAD (23) to investigate CAD cluster formation as a read-out for C-terminal STIM1 oligomerization (Fig. S5 A–D). Whereas WT YFP-TMG-CAD proteins readily formed clusters, cluster formation was significantly impaired for mutant (R429C) YFP-TMG-CAD (Fig. S5 A–D). Taken together, our data show that R429 regulates the C-terminal oligomerization of STIM1 dimers.

R429 Regulates STIM1 Puncta Formation and Colocalization with ORAI1. A visible consequence of STIM1 oligomerization is the formation of STIM1 puncta at ER–PM junctions (5, 24, 25). We analyzed the role of R429 and CC3 for STIM1 puncta formation by time-lapse total internal reflection fluorescence microscopy (TIRFM) in cells expressing WT or mutant (R429C) mCherry-STIM1 together with GFP-ORAI1. In nonstimulated cells, STIM1-WT localized to the bulk ER away from the PM and was invisible by TIRFM whereas ORAI1 was distributed homogeneously in the PM (Fig. 5A). After ER store depletion with TG, STIM1-WT formed puncta, translocated to ER-PM junctions within the TIRF evanescent field, and colocalized with ORAI1 (Fig. 5A, C, and D). Surprisingly, mutant STIM1-R429C was already localized near the PM in cells, with filled ER Ca²⁺ stores forming large, plaque-like structures (Fig. 5B). Upon store depletion, STIM1-R429C did not change its distribution and failed to redistribute into discrete puncta (Fig. 5B and C). In addition, the distribution of GFP-ORAI1 remained homogenous after store depletion without signs of puncta formation and no significant colocalization with mCherry-STIM1-R429C (Fig. 5B and D). This finding is consistent with the known role of STIM1 in recruiting ORAI1 into puncta and the impaired binding of mutant STIM1 to ORAI1 (Fig. 2). Similar results were obtained in cells overexpressing R429E and R429L mutants (Fig. 5C). The aberrant localization of mutant STIM1-R429C to ER–PM junctions is not an overexpression artifact because endogenous STIM1-R429C protein in nonstimulated patient T cells also localized close to the PM and failed to form discrete puncta after

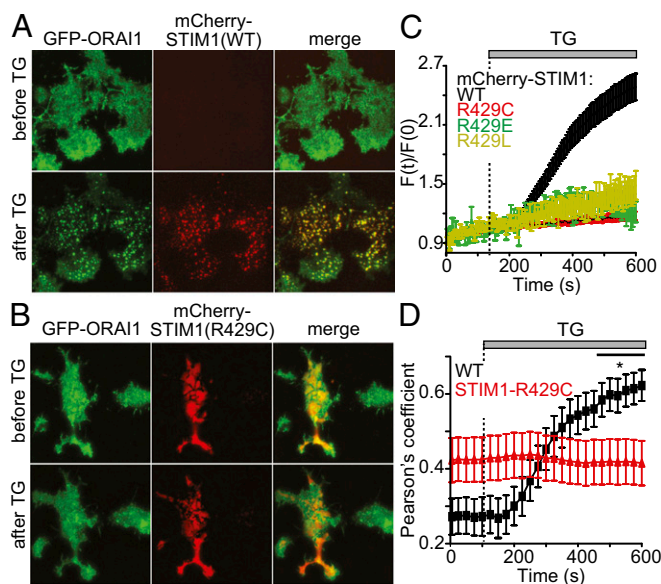


Fig. 5. R429 regulates STIM1 puncta formation and colocalization with ORAI1. (A and B) Representative total internal reflection microscopy (TIRFM) images of HEK293 cells expressing GFP-ORAI1 and WT or mutant (R429C) mCherry-STIM1 before and after stimulation with 1 μ M TG in Ca²⁺-free Ringer's solution for 10 min. (C) Relative fluorescence $[F(t)/F_0]$ of WT and mutant (R429C, R429E, or R429L) mCherry-STIM1 in the TIRFM evanescent field. (D) Colocalization between GFP-ORAI1 and WT or mutant (R429C) mCherry-STIM1 was measured by determining the Pearson's coefficient for GFP and mCherry signals. Traces in C and D represent averages \pm SEM ($n > 35$ cells). Data are representative of five repeat experiments. * $P < 0.05$.

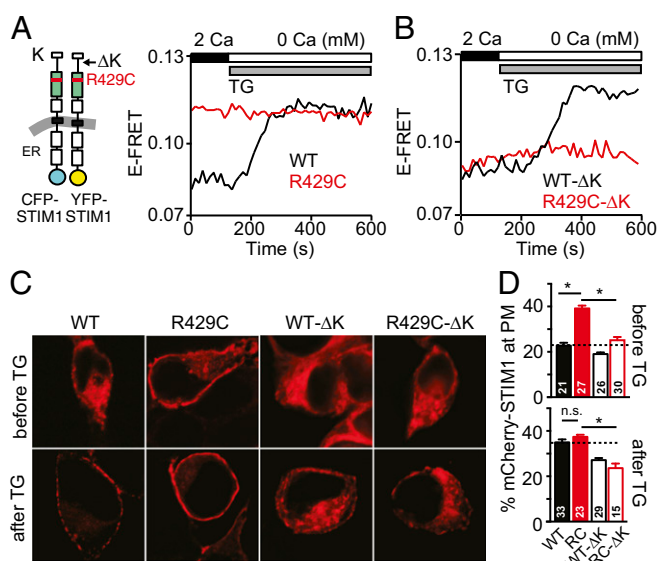


Fig. 6. R429C controls exposure of the polybasic domain and STIM1 oligomerization. (A and B) Representative traces showing E-FRET between WT or mutant (R429C) CFP-STIM1 and YFP-STIM1 that either contain (A) or lack (Δ K in B) the K-rich polybasic domain. To induce STIM1 oligomerization, HEK293 cells were stimulated with 1 μ M TG in Ca²⁺-free Ringer's solution. Summary and statistical analysis of E-FRET data in Fig. S7 A–C. (C) Representative confocal images of WT or mutant (R429C) mCherry-STIM1 containing or lacking (Δ K) the polybasic domain in HEK293 cells before, and 8 min after, stimulation with 1 μ M TG. (D) mCherry-STIM1 fluorescence in the vicinity of the PM as a percentage of total mCherry fluorescence from experiments in C. Number of cells analyzed as indicated. * $P < 0.05$. Supporting information in Fig. S7.

store depletion (Fig. S5 E and F). We further excluded that constitutive localization of mutant STIM1 at ER-PM junctions is due to its insertion into the PM (Fig. S6). Collectively, our data show that mutation of R429 results in constitutive STIM1 localization in the junctional ER, thus uncoupling STIM1 translocation from the filling state of ER Ca²⁺ stores. However, despite its localization at ER–PM junctions, mutant STIM1 fails to form discrete puncta, likely due to its impaired ability to oligomerize.

R429 Is Required for Store Depletion-Induced Homotypic STIM1-CT Oligomerization. To further investigate the role of R429 and CC3 in STIM1 oligomerization in live cells, we measured FRET between STIM1 proteins (22). In cells expressing N-terminally tagged YFP-STIM1-WT and CFP-STIM1-WT, we observed a robust increase in E-FRET after TG stimulation compared with cells with filled Ca²⁺ stores due to STIM1 oligomerization (Fig. 6A and Fig. S7 A and C), similar to previous studies (13, 22). By contrast, store depletion in cells expressing mutant CFP-STIM1-R429C and YFP-STIM1-R429C did not induce an E-FRET increase consistent with impaired oligomerization and formation of discrete puncta described above (Figs. 4 and 5). Surprisingly, baseline E-FRET levels between mutant proteins were significantly elevated (Fig. 6A and Fig. S7 A and C). We hypothesized that increased E-FRET may be due to constitutive and store-independent low affinity interactions between mutant STIM1-R429C molecules at spatially constrained ER–PM junctions with high STIM1 concentrations. Recruitment of STIM1 to ER–PM junctions is dependent on the binding of the C-terminal polybasic domain of STIM1 (amino acids 675–685) to negatively charged PM phospholipids (11, 13). Deletion of the polybasic domain (Δ K) in STIM1-WT had no effect on either baseline E-FRET or the E-FRET increase after store depletion (Fig. 6B and Fig. S7 B and C). By contrast, its deletion in mutant STIM1-R429C reduced baseline E-FRET to levels observed with STIM1-WT. It did not restore, however, the impaired increase in E-FRET seen with STIM1-R429C after store depletion (Fig. 6B and

Fig. S7 B and C). Together, these data provide further evidence that mutation of R429 abolishes store depletion-induced STIM1 oligomerization.

R429 Regulates the Transition of STIM1 from a Closed to Open Conformation. The constitutive localization of STIM1-R429C at ER-PM junctions and the increased baseline E-FRET between STIM1-R429C proteins suggest that R429 controls the exposure of the polybasic domain (9–11). Indeed, deletion of the polybasic domain resulted in the redistribution of STIM1-R429C-ΔK to the bulk ER whereas STIM1-R429C was constitutively present at ER-PM junctions (Fig. 6 C and D), suggesting that R429 indeed controls exposure of the polybasic domain and thereby STIM1 recruitment to the PM. Deletion of the polybasic domain did not, however, restore the ability of STIM1-R429C-ΔK to activate SOCE (Fig. S7 D and E). To further test whether R429 regulates conformational changes of the STIM1-CT, we used a FRET-based conformational sensor, in which the ORAI1-activating small fragment (OASF, amino acids 233–474) of STIM1 is flanked by CFP and YFP (10). The WT OASF sensor exhibited robust intramolecular FRET indicative of a closed OASF conformation as previously described (Fig. 7) (10). By contrast, substitution of R429 with C, E, L, or K significantly reduced intramolecular FRET (Fig. 7B and Fig. S8A), suggesting that mutation of R429 results in an extended conformation of OASF. It is noteworthy that mutant OASF-R429C, in contrast to OASF-WT, did not colocalize with coexpressed ORAI1, consistent with its impaired binding to ORAI1 (Fig. S8B). Taken together, our data demonstrate that R429 in CC3 is essential for maintaining the closed conformation of quiescent STIM1 and thereby regulating the translocation of STIM1 to ER-PM junctions via its polybasic domain.

R429 Stabilizes the α -Helical Structure of CC3. Our data show that mutation of R429 impairs several critical STIM1 functions. We hypothesized that R429 regulates all these STIM1 functions by maintaining a stable CC3 fold. We therefore analyzed the effects of R429 mutations on the structure and stability of STIM1 cytosolic domains by recombinantly expressing mutant and WT STIM1 fragments. Analysis of the far-UV circular dichroism (CD) spectra of STIM1 fragments that encompass all three CC domains (amino acids 234–491) showed that WT and mutant proteins are primarily α -helical. However, the α -helicity of mutant proteins (R429C, R429A, or R429L) was reduced by ~8–9% compared with WT protein (Fig. 8A). We also assessed the stability of the mutant proteins by monitoring the fractional changes in far-UV CD signals as a function of temperature. An overlay of the thermal melt curves showed marked (~10–13 °C) shifts to lower temperatures in the midpoints of temperature denaturation (T_m) for mutant (R429A, R429L, and R429C) compared to WT proteins (Fig. 8B and Fig. S3C) indicating that mutant proteins are less stable. Together, these data indicate that R429 is critical for supporting a stable α -helical fold of CC3,

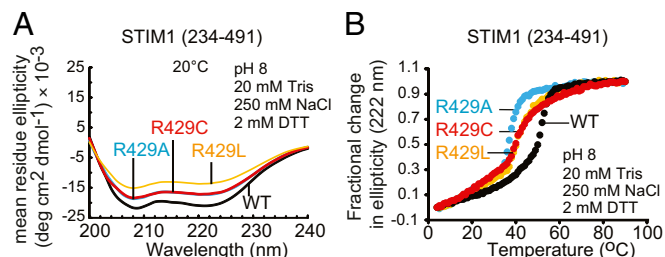


Fig. 8. R429 stabilizes α -helical structure of CC3. (A) α -Helicity of recombinant WT and mutant (R429C, R429A, R429L) C-terminal STIM1 fragments (amino acids 234–491) measured by far-UV CD spectra (200–240 nm). (B) Thermal stability of WT and mutant STIM1 fragments determined from the normalized fractional change in ellipticity at 222 nm over a temperature range of 4–90 °C. Experimental conditions are indicated in the figure. Summary of results and Supporting information in Fig. S3.

which is a plausible explanation for how R429 regulates intra- and intermolecular STIM1 interactions and multiple STIM1 functions.

Discussion

We here elucidate the molecular mechanisms by which a loss-of-function mutation (R429C) in STIM1 abolishes SOCE in immunodeficient patients, thereby demonstrating multiple important roles of the CC3 domain in which R429 is located. We find that R429 enables CC3 to regulate (i) the transition of STIM1-CT from a closed, inactive to an extended, active conformation, (ii) the formation of higher order STIM1-CT oligomers, and (iii) the binding of STIM1 to ORAI1 (Fig. 9).

The C terminus of STIM1 adopts an inactive conformation in cells with filled Ca²⁺ stores (9–11, 21) and undergoes a conformational extension upon ER store depletion, allowing STIM1 to bridge the gap between the ER and PM. The molecular mechanisms controlling this transition are incompletely understood but were proposed to involve hydrophobic (10) and electrostatic interactions (9, 21, 26) between the CC1 and CC2 domains of STIM1-CT. The role of CC1 in maintaining STIM1-CT in a closed, inactive conformation has been demonstrated by in vitro studies (10, 11) and is emphasized by recent reports identifying a gain-of-function mutation in CC1 (R304W) as the cause of Stormorken syndrome (27–29). Our studies of the R429C patient mutation highlight a hitherto unappreciated role for CC3 in addition to CC1 in maintaining the inactive conformation of STIM1, as mutant STIM1-R429C adopts a constitutively open conformation and localizes to ER-PM junctions independently of ER store Ca²⁺ content. In this respect, it behaves similarly to the previously described L416S and L423S mutations in CC3 (10); however, whereas L416S and L423S mutations cause constitutive CRAC channel activation, R429C abolishes SOCE, demonstrating that CC3 has additional important roles in STIM1 function.

In cells with filled ER Ca²⁺ stores, STIM1 was suggested to exist in dimers (17, 18). The crystal structure of the human SOAR domain (amino acids 344–442) shows a dimer that is stabilized by hydrophobic and charged interactions involving R429 (17). In our experiments, mutation of R429, however, does not interfere with the dimerization of C-terminal STIM1 domains as demonstrated by FRET and SEC-MALS analyses. By contrast, we here show that R429 is required for the assembly of STIM1-CT dimers into higher order oligomers as demonstrated by impaired store depletion-induced STIM1-STIM1 FRET, loss of co-IP between mutant (R429C) STIM1 dimers, reduced formation of high molecular weight complexes of STIM1-R429C in BN-PAGE, and impaired puncta formation of full-length STIM1 and CAD. Puncta formation is a hallmark of SOCE and depends on oligomerization of the N and C termini of STIM1. Oligomerization requires CAD because truncated STIM1 proteins lacking CAD fail to properly oligomerize upon ER store depletion

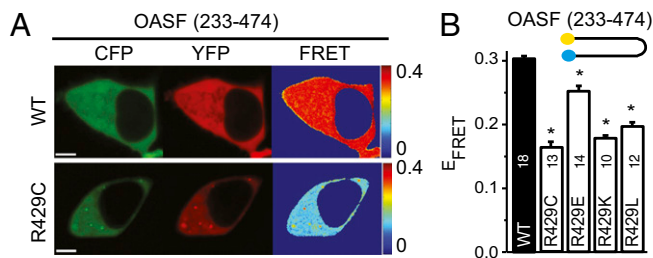


Fig. 7. R429 maintains STIM1 in closed conformation. (A) Representative confocal microscopy images of YFP, CFP, and FRET signals from the WT or mutant (R429C) YFP-OASF-CFP (amino acids 233–474) intramolecular FRET-sensor expressed in HEK293 cells. (B) Averaged resting E-FRET levels of WT and mutant (R429C, R429E, R429K, or R429L) YFP-OASF-CFP in nonstimulated cells. Number of cells analyzed as indicated. * $P < 0.05$. Supporting information in Fig. S8.

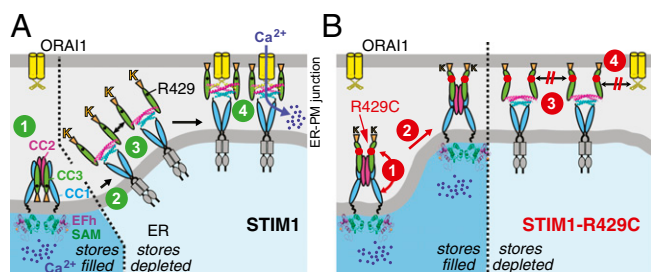


Fig. 9. Model of STIM1 activation and effects of R429 mutation in CC3. (A) In cells with filled ER Ca^{2+} stores, STIM1-CT exists in a closed conformation that is maintained by R429 and CC3 (step 1). After store depletion, STIM1-CT undergoes a CC3-dependent conformational change, resulting in an exposed polybasic domain and STIM1 translocation to ER-PM junctions (step 2), oligomerization (step 3), and ORAI1 binding (step 4). (B) Mutant STIM1-R429C has an extended conformation with exposed polybasic domain (step 1) and is constitutively localized at ER-PM junctions (step 2), but fails to oligomerize (step 3) and bind to ORAI1 (step 4) due to the destabilized CC3 structure.

(13, 18, 25, 30). We show here that oligomerization of CAD depends on R429 because cluster formation of ER membrane-tethered mutant CAD proteins is impaired compared with WT CAD. When expressed as full-length protein, STIM1-R429 is localized in large, plaque-like structures that likely represent ER-PM junctions to which mutant STIM1 is recruited via its extended C terminus and exposed polybasic domain that allow it to interact with PM phospholipids (11, 13). Upon store depletion, STIM1-R429C remains homogeneously distributed within the entire junctional ER area and fails to aggregate into discrete puncta. This abnormal distribution is likely due to its inability to oligomerize, consistent with its impaired formation of high molecular weight complexes in BN-PAGE. The plaque-like distribution of STIM1-R429C and impaired puncta formation is in contrast to activating mutations in the CC1 domain of STIM1, such as L251S, which, despite its extended C terminus, does not result in a plaque-like distribution (10, 11) because it retains the ability to oligomerize and form discrete puncta within the available junctional ER area.

CAD was shown to bind ORAI1 and activate the CRAC channel (14–16). We here demonstrate that R429 and CC3 are critical for the interaction of CAD with ORAI1 because mutation of R429 abolishes PM localization of CAD and OASF proteins, FRET between CAD and ORAI1, and CAD (CCb9)-mediated Ca^{2+} influx. Whereas several residues in CC2 were shown to mediate CAD interactions with ORAI1 (9, 10, 18, 26), including A376 (18) and a hydrophobic STIM1-ORAI1 association pocket (SOAP) we recently identified by NMR structure analysis (19), a similar role for CC3 has not been reported. The exact mechanism by which R429 and CC3 regulate the binding of STIM1 to ORAI1 remains unclear at present and awaits high resolution structural data of the STIM1-CC3 and ORAI1 complex. It is conceivable that STIM1-CC3 binds to the N terminus of ORAI1 instead of its C terminus, consistent with the reported binding of STIM1 to the N and C terminus of ORAI1 for proper CRAC channel gating (14, 31). Alternatively, CC3 may enhance the interaction of STIM1-CC2 and ORAI1 via the intersubunit CC3–CC3' interaction we proposed earlier (19). Irrespective of the precise nature of this interaction, the present study provides compelling evidence that the CC3 domain is required for STIM1 binding to ORAI1 and CRAC channel activation.

Materials and Methods

SI Materials and Methods includes detailed descriptions of all methods and materials used. Informed consent for studies using patient cells was obtained from the patient's family in accordance with the Declaration of Helsinki and Institutional Review Board approval from the University of Freiburg and New York University School of Medicine.

ACKNOWLEDGMENTS. We thank Drs. R. S. Lewis, T. Meyer, T. Shuttleworth, and M. Oh-hora for providing reagents and members of our laboratories for valuable discussions. This work was funded by grants from the National Institutes of Health [NIH Grants A1097302 (to S. Feske) and NS057499 (to M.P.)], the Canadian Institutes of Health Research and the Heart and Stroke Foundation of Canada (to M.I.), the Natural Sciences and Engineering Research Council of Canada (to P.B.S.), the Austrian Science Fund [FWF Projects P25172 and P27263 (to C.R.)], and the Bundesministerium für Bildung und Forschung [BMBF Grant 01EO1303 (to S.E.)] and by Deutsche Forschungsgemeinschaft Postdoctoral Fellowship We 5303/1-1 (to C.W.).

- Feske S, et al. (2006) A mutation in Orai1 causes immune deficiency by abrogating CRAC channel function. *Nature* 441(7090):179–185.
- Vig M, et al. (2006) CRACM1 is a plasma membrane protein essential for store-operated Ca^{2+} entry. *Science* 312(5777):1220–1223.
- Zhang SL, et al. (2006) Genome-wide RNAi screen of Ca^{2+} influx identifies genes that regulate Ca^{2+} release-activated Ca^{2+} channel activity. *Proc Natl Acad Sci USA* 103(24):9357–9362.
- Shaw PJ, Qu B, Hoth M, Feske S (2013) Molecular regulation of CRAC channels and their role in lymphocyte function. *Cell Mol Life Sci* 70(15):2637–2656.
- Liou J, et al. (2005) STIM1 is a Ca^{2+} sensor essential for Ca^{2+} -store-depletion-triggered Ca^{2+} influx. *Curr Biol* 15(13):1235–1241.
- Roos J, et al. (2005) STIM1, an essential and conserved component of store-operated Ca^{2+} channel function. *J Cell Biol* 169(3):435–445.
- Feske S (2011) Immunodeficiency due to defects in store-operated calcium entry. *Ann N Y Acad Sci* 1238:74–90.
- Hogan PG, Lewis RS, Rao A (2010) Molecular basis of calcium signaling in lymphocytes: STIM and ORAI. *Annu Rev Immunol* 28:491–533.
- Korzeniowski MK, Manjarrés IM, Varnai P, Balla T (2010) Activation of STIM1-Orai1 involves an intramolecular switching mechanism. *Sci Signal* 3(148):ra82.
- Muik M, et al. (2011) STIM1 couples to ORAI1 via an intramolecular transition into an extended conformation. *EMBO J* 30(9):1678–1689.
- Zhou Y, et al. (2013) Initial activation of STIM1, the regulator of store-operated calcium entry. *Nat Struct Mol Biol* 20(8):973–981.
- Yu F, Sun L, Hubrack S, Selvaraj S, Machaca K (2013) Intramolecular shielding maintains the ER Ca^{2+} sensor STIM1 in an inactive conformation. *J Cell Sci* 126(Pt 11):2401–2410.
- Liou J, Fivaz M, Inoue T, Meyer T (2007) Live-cell imaging reveals sequential oligomerization and local plasma membrane targeting of stromal interaction molecule 1 after Ca^{2+} store depletion. *Proc Natl Acad Sci USA* 104(22):9301–9306.
- Park CY, et al. (2009) STIM1 clusters and activates CRAC channels via direct binding of a cytosolic domain to Orai1. *Cell* 136(5):876–890.
- Yuan JP, et al. (2009) SOAR and the polybasic STIM1 domains gate and regulate Orai channels. *Nat Cell Biol* 11(3):337–343.
- Kawasaki T, Lange I, Feske S (2009) A minimal regulatory domain in the C terminus of STIM1 binds to and activates ORAI1 CRAC channels. *Biochem Biophys Res Commun* 385(1):49–54.
- Yang X, Jin H, Cai X, Li S, Shen Y (2012) Structural and mechanistic insights into the activation of stromal interaction molecule 1 (STIM1). *Proc Natl Acad Sci USA* 109(15):5657–5662.
- Covington ED, Wu MM, Lewis RS (2010) Essential role for the CRAC activation domain in store-dependent oligomerization of STIM1. *Mol Biol Cell* 21(11):1897–1907.
- Stathopoulos PB, et al. (2013) STIM1/Orai1 coiled-coil interplay in the regulation of store-operated calcium entry. *Nat Commun* 4:2963.
- Fuchs S, et al. (2012) Antiviral and regulatory T cell immunity in a patient with stromal interaction molecule 1 deficiency. *J Immunol* 188(3):1523–1533.
- Calloway N, Vig M, Kinet JP, Holowka D, Baird B (2009) Molecular clustering of STIM1 with Orai1/CRACM1 at the plasma membrane depends dynamically on depletion of Ca^{2+} stores and on electrostatic interactions. *Mol Biol Cell* 20(11):389–399.
- Navarro-Borely L, et al. (2008) STIM1-Orai1 interactions and Orai1 conformational changes revealed by live-cell FRET microscopy. *J Physiol* 586(Pt 22):5383–5401.
- Fahrner M, et al. (2014) A coiled-coil clamp controls both conformation and clustering of stromal interaction molecule 1 (STIM1). *J Biol Chem* 289(48):33231–33244.
- Luik RM, Wu MM, Buchanan J, Lewis RS (2006) The elementary unit of store-operated Ca^{2+} entry: Local activation of CRAC channels by STIM1 at ER-plasma membrane junctions. *J Cell Biol* 174(6):815–825.
- Wu MM, Buchanan J, Luik RM, Lewis RS (2006) Ca^{2+} store depletion causes STIM1 to accumulate in ER regions closely associated with the plasma membrane. *J Cell Biol* 174(6):803–813.
- Calloway N, Holowka D, Baird B (2010) A basic sequence in STIM1 promotes Ca^{2+} influx by interacting with the C-terminal acidic coiled coil of Orai1. *Biochemistry* 49(6):1067–1071.
- Misceo D, et al. (2014) A dominant STIM1 mutation causes Stormorken syndrome. *Hum Mutat* 35(5):556–564.
- Nesin V, et al. (2014) Activating mutations in STIM1 and ORAI1 cause overlapping syndromes of tubular myopathy and congenital myosis. *Proc Natl Acad Sci USA* 111(11):4197–4202.
- Morin G, et al. (2014) Gain-of-function mutation in STIM1 (P.R304W) is associated with Stormorken syndrome. *Hum Mutat* 35(10):1221–1232.
- Muik M, et al. (2009) A cytosolic homomerization and a modulatory domain within STIM1 C terminus determine coupling to ORAI1 channels. *J Biol Chem* 284(13):8421–8426.
- Zhou Y, et al. (2010) STIM1 gates the store-operated calcium channel ORAI1 in vitro. *Nat Struct Mol Biol* 17(1):112–116.